Chemokines in Ewing sarcoma

Sand, L.G.L.

Citation

Sand, L. G. L. (2016, October 27). *Chemokines in Ewing sarcoma*. Retrieved from https://hdl.handle.net/1887/43794

Cover Page

Universiteit Leiden

Chapter 4

CXCL14, CXCR7 expression and *CXCR4* splice variant ratio associate with survival and metastases in Ewing sarcoma patients

L.G.L. Sand, K. Scotlandi, D. Berghuis, B.E. Snaar-Jagalska, P. Picci, T. Schmidt, K. Szuhai and P.C.W. Hogendoorn

ABSTRACT

Ewing sarcoma (EWS) is the second most common sarcoma of bone in children and young adults. Patients with disseminated disease at diagnosis or early relapse have a poor prognosis. Our goal was to identify novel predictive biomarkers for these patients, focusing on chemokines, specifically genes involved in the CXCR4-pathway because of their established role in metastasis and tumor growth.

Total RNA isolated from therapy-naïve tumor samples (n = 18; panel I) and cell lines (n = 21) was used to study expression of CXCR4-pathway related genes and CXCR4 splice variants (*CXCR4-2* and *CXCR4-1*) by RT-Q-PCR. *CXCL12, CXCR4, CXCR7* and *CXCL14*, and both splice variants were expressed in cell lines and tumor samples. *CXCR4-1/CXCR4-2* ratio was significantly higher in tumor samples compared to cell lines and showed a positive correlation with overall survival (OS) and event free survival (EFS). In addition, high *CXCR7* and *CXCL14* expression levels were correlated with improved EFS and OS and negatively correlated with metastasis development. The results from the test panel were validated in an independent sample panel. This identified set of genes which are involved in CXCR4 signaling might be used as a marker to predict survival and metastasis development in Ewing sarcoma.

KEYWORDS

Splice variant; Tumor microenvironment; Biomarker; Molecular targeted therapy

INTRODUCTION

Ewing sarcoma (EWS) is the second most common bone neoplasm in children and young adolescents while soft tissue and organ related involvement is more often observed in adults [1]. Genetically, EWS is characterized by a recurrent translocation of the *EWSR1* gene to a member of the family of ETS transcription factors [1-2]. Rarely, tumors with Ewing sarcoma-like features exist were *EWSR1* is fused to a non-ETS family member or between BCOR–CCNB3 or CIC–DUX4 genes [1, 3-5].

The introduction of multi-agent chemotherapy in combination with advancements in surgery and radiotherapy has improved the 5-year overall survival (OS) of EWS patients with localized disease from less than 10–70% nowadays, irrespective of the type of classical Ewing sarcoma specific translocation [6-7]. However, the OS drops to less than 30% when metastases are present at the time of diagnosis which is the case in 15–30% of new presentations- or with tumor relapse [8-9]. For these high risk patients many markers have been suggested, but at present only classical markers, such as tumor location, are used in clinic [10]. EWS is recognized from the onset of its original description by James Ewing as a highly vascularized tumor and amongst many other pathways, chemokine and the TGF-B pathway might play a role for this excessive vascularization pattern [11-13]. Besides angiogenesis, these pathways are involved in migration that might be reflected by the high metastatic propensity of EWS [1], 13, 14]. In several tumor types a positive correlation between increased expression of CXCR4 and metastatic propensity was reported, but contradictory results were reported in EWS [15], [16] and [17].

CXCR4 is a chemokine receptor from the G-protein coupled receptor family binding the CXC chemokines. CXCR4 ligands are chemokine CXCL12, also known as stromal cell-de-

rived factor 1 (SDF1) and CXCL14, also known as BRAK [18-19].

For *CXCR4* two common splice variants have been described in humans by Gupta et al. containing either two exons *CXCR4-2* or one exon by utilizing another transcription initiation code inside intron one *CXCR4-1* [20]. At the protein level, the first five amino acids at the N-terminus of CXCR4-2 are replaced with nine amino acids in the CXCR4-1 variant. Hence, the N-terminal part of CXCR4 is crucial in CXCL12 binding therefore this change may interfere with CXCR4 activation [20-21]. The expression levels of these two splice variants have neither been studied in tumor samples nor associated with survival.

To study the role of different chemokines and their receptors in combination with the detection of different *CXCR4* isoforms we performed whole transcriptome RNA sequencing and a real-time quantitative-reverse transcriptase PCR (RT-Q-PCR) on EWS cell lines and two panels of therapy-naïve tumor samples (test and a validation set: panel I and panel II). Results of the RT-Q-PCR were correlated to clinical parameters. Survival analysis of panel I showed that high *CXCR4-1* over *CXCR4-2* ratio and high expression of *CXCL14* and *CXCR7* positively correlated with EFS and OS. These findings were overall confirmed by a validation set (panel II). Thus, *CXCL14, CXCR7* and the ratio between *CXCR4-2* and *CXCR4-1* could predict EFS and OS in Ewing sarcoma patients, which is probably related to their role in CXCR4 signaling pathway.

MATERIAL AND METHODS

Clinical information patient samples

Ewing sarcoma diagnosis was established according to World Health Organization (WHO) criteria, including immunohistochemistry and *EWSR1* translocation detection either by RT-Q-PCR or interphase FISH. 18 cryopreserved therapy-naïve samples from 18 patients containing at least 80% tumor were collected at the Department of Pathology, Leiden University Medical Center (**Table 1A; panel I**). Median patient age at diagnosis was 17.5 years (range of 5–35 years). All patient samples were handled in a coded fashion, according to the Dutch national ethical guidelines ('Code for Proper Secondary Use of Human Tissue', Dutch Federation of Medical Scientific Societies). For validation a panel of 25 cryopreserved therapy-naïve samples from 25 patients were obtained from the Rizzoli Orthopedics Institute with a median age at diagnosis of 16 years (range 3–45 years) (**Table 1B; panel II**).

Ewing sarcoma cell lines

21 Ewing sarcoma cell lines were obtained from multiple sources: L-1062 and L-872 were established in-house; SK-ES-1, SK-NM-C, A-673 and R-D-ES from the American Type Culture Collection and CHP100, RM-82, IARC-EW-7, WE-68, IARC-EW-3, STA-ET-2.1, TTC-466, TC-32, STA-ET-10, CADO-ES1, STA-ET-1, TC-71, COH and VH-64 were obtained from the EuroBoNET consortium collection located at the Institute of Pathology, University Medical Center, Düsseldorf, Germany; 6647 was kindly was kindly provided by Dr. Timothy Triche (CHLA, Los Angeles, CA, USA). All cell lines and primary culture L-4027 were cultured in Iscove's Modified Dulbecco's Medium containing GlutaMAX supplement, supplemented with 1% streptomycin/penicillin and 10% heat-inactivated FCS (all from Life Technologies, Bleiswijk, The Netherlands). Regular Mycoplasma DNA Q-PCR screening [22] and authentication of cell lines using Powerplex 1.2 and CellID STR (Promega, Leiden, The Netherlands) were performed on all cell lines.

Table 1: Clinical details of the two study panels

Table1a: Clinical details of patients in study panel I

Patient number	Age (years)	Sex	Primary tumor site	Ex-tremi-ty[a]	Pelvic[b]	Starting treatment protocol	Tumor volume[c]	Neoad-juvant chemo-therapy[d]	Neoadju-vant Radio-therapy[e]
L318	35	male	prox radius	1	0	CESS86	ND	1	0
L463	24	male	thorax wall	0	0	CESS86	ND	0	0
L469	19	female	distal fibula	1	0	EICESS	1	1	0
L513	11	male	pelvis	0	1	EICESS	1	ND	1
L629	5	male	tibia + fibula	1	0	EuroEwing99	1	1	0
L683	17	male	tibia	1	0	EICESS	ND	1	0
L848	15	female	humerus	1	0	EuroEwing99	0	1	0
L1034	18	male	pelvis	0	1	EuroEwing99	1	1	0
L1098	10	male	femur	1	0	EuroEwing99	0	1	0
L1220	19	male	os pubis	0	1	EuroEwing99	1	1	-
L1232	14	male	humerus	1	0	EuroEwing99	ND	ND	0
L1379	13	male	fibula	1	0	EuroEwing99	ND	1	0
L1489	25	male	pelvis	0	1	EuroEwing99	1	1	1
L1570	12	male	humerus	1	0	EuroEwing99	ND	1	0
L1722	18	male	humerus	1	0	EuroEwing99	1	1	0
L2154	11	female	femur	1	0	EuroEwing99	0	1	-
L2161	19	male	pelvis	0	1	EuroEwing99	1	1	0
L2162	19	male	pelvis	0	1	EuroEwing99	1	1	0

ND: Not determined

EFS: Event free survival

OS: overall survival

[a,b,d,e,f,g,I,k,j] **1**: event reported or **0**: no event reported

[c] **1** tumor volume > 200 ml or **0**: < 200 ml

[h] **1**: < 10% tumor vitality or **0**: > 10% tumor vitality

[b] **1**: Dead or **0**: alive.

Surgery[f]	Resectable with free margins[g]	Response to chemo-therapy[h]	Metas-tasis at diagnosis[i]	Metas-tasis later[j]	Local re-currence/ Relapse[k]	EFS Time (month)	EFS[l]	OS Time (month)	OS[m]
1	1	1	0	0	0	183	0	233	0
1	1	ND	0	1	1	12	1	20	1
1	0	0	0	1	1	20	1	23	1
0	-	ND	1	0	ND	18	1	18	1
1	1	1	1	0	0	135	0	135	0
1	0	0	0	1	0	10	1	16	1
1	1	1	1	0	0	142	0	142	0
1	0	0	1	1	0	11	1	18	1
1	0	1	0	0	0	129	0	129	0
0		ND	1	1	0	10	1	11	1
1	1	ND	0	0	ND	14	1	34	1
1	1	0	1	0	0	99	0	99	0
1	1	1	0	0	0	91	0	91	0
1	1	1	0	0	0	83	0	83	0
1	1	1	0	1	1	36	1	36	0
1	1	1	1	0	0	176	0	176	0
0	-	0	0	1	0	11	1	12	1
0	-	ND	1	1	0	15	1	19	1

4

Table 1b: Clinical details of patients in validation panel II

Patient number	Age (years)	Sex	Primary tumor site	Ex-tremity[a]	Pelvic[b]	Starting treatment protocol	Tumor volume[c]	Neoad-juvant chemo-therapy[d]	Neoadju-vant Radio-therapy[e]
R040	24	male	femur	1	0	IOR NEO3	1	1	0
R042	18	male	femur	1	0	IOR NEO3	0	1	0
R046	7	female	radius	1	0	IOR NEO3	0	1	0
R060	12	male	pelvis	0	1	IOR NEO3	0	1	1
R063	13	male	pelvis	0	1	ISG-SSG3	0	1	1
R078	11	female	pelvis	0	1	ISG-SSG4	1	1	1
R080	8	female	femur	1	0	ISG-SSG3	0	1	0
R517	3	male	humerus	1	0	ISG-SSG PILOT	0	1	0
R650	26	female	femur	1	0	ISG-SSG3	0	1	0
R653	9	male	tibia	1	0	ISG-SSG4	0	1	0
R658	17	female	tibia	1	0	IOR NEO2	0	1	1
R673	15	female	humerus	1	0	ISG-SSG3	0	1	0
R680	17	male	fibula	1	0	ISG-SSG3	0	1	0
R681	12	female	femur	1	0	ISG-SSG3	0	1	0
R822	31	male	tibia	1	0	ISG-SSG3	0	1	0
R833	17	female	femur	1	0	ISG-SSG3	0	1	0
R835	26	male	scapula	1	0	ISG-SSG3	0	1	0
R863	18	male	tibia	1	0	ISG-SSG3	0	1	0
R880	10	male	radius	1	0	ISG-AIEOP	0	1	0
R891	21	male	femur	1	0	ISG-SSG3	0	1	0
R892	37	female	femur	1	0	ISG-AIEOP	1	1	0
R906	10	male	humerus	1	0	ISG-AIEOP	1	1	0
R910	45	male	scapula	1	0	ISG-AIEOP	1	1	0
R914	10	male	femur	1	0	EUROEW-ING99	0	1	0
R917	14	male	metatarsus	1	0	ISG-AIEOP	1	1	0

ND: Not determined

EFS: Event free survival

OS: overall survival

[a,b,d,e,f,g,I,k,j] **1**: event reported or **0**: no event reported

[c] **1** tumor volume > 200 ml or **0**: < 200 ml

[h] **1**: < 10% tumor vitality or **0**: > 10% tumor vitality

[b] **1**: Dead or **0**: alive

Surgery[f]	Resectable with free margins[g]	Response to chemo-therapy[h]	Metas-tasis at diagnosis[i]	Metas-tasis later[j]	Local re-currence/ Relapse[k]	EFS Time (month)	EFS[l]	OS Time (month)	OS[m]
1	1	0	0	1	0	17	1	135	0
1	1	0	0	0	0	262	0	262	0
1	1	0	0	1	0	21	1	63	1
0	ND	ND	0	0	0	226	0	226	0
0	ND	ND	0	0	0	109	0	109	0
0	ND	ND	1	0	0	183	0	183	0
1	0	0	0	1	0	57	1	72	1
1	0	0	0	0	0	161	0	161	0
1	0	0	0	1	0	28	1	141	0
1	1	1	1	1	0	30	1	52	1
0	ND	ND	0	1	1	24	1	35	1
1	1	1	0	0	0	122	0	122	0
1	1	1	0	0	0	122	0	122	0
1	1	1	0	0	0	151	0	151	0
1	1	0	0	1	0	11	1	21	1
1	1	0	0	1	0	43	1	63	1
1	1	0	0	0	0	128	0	128	0
1	1	0	0	0	0	106	0	106	0
1	1	1	0	0	0	84	0	84	0
1	1	0	0	0	0	89	0	89	0
1	1	0	0	0	0	84	0	84	0
1	0	0	0	1	0	12	1	25	1
1	1	0	0	1	0	19	1	33	1
1	1	0	0	1	0	52	1	64	1
1	1	1	1	0	0	59	0	59	0

4

RNA isolation

Total RNA was isolated using TRIzol Reagent (Life Technologies, Bleiswijk, The Netherlands) according to manufacturer's instruction. RNA concentration was measured using Nanodrop and quality of the RNA was determined using Bioanalyzer2000 RNA Nano chip (Agilent Technology, Amstelveen, The Netherlands). For whole transcriptome RNA sequencing analysis a RNA Integrity Number (RIN) of 8 was set as threshold. For the RT-Q-PCR analysis the inclusion criteria were at least a RIN of 5 and measurable expression levels.

CXCR4 splice variant specific primer design and detection

CXCR4 splice variant specific primers sets were designed for RT-Q-PCR based expression analysis. *CXCR4-2* primers CXCR4-2F 5'AGGTAGCAAAGTGACGCCGA 3' and CXCR4-2R 5' TAGTCCCCTGAGCCCATTTCC 3' were intron spanning by priming exon 1 and exon 2. *CXCR4-1* primers were CXCR4-1F 5' GACTTTGAAACCCTCAGCGTC 3' and CXCR4-1R 5' TCCTACAACTCTCCTCCCCAT 3'. Products were detected by using 10ul RT-Q-PCR mixture using iQ SYBR Green supermix (Biorad, Hercules, CA, USA).

RT-Q-PCR analysis and Fluidigm

cDNA generation and RT-Q-PCR using Fluidigm biomark system was performed according to the H format instructions of the manufacturer (QIAGEN, Venlo, The Netherlands). Samples were prepared for RT-Q-PCR using a 96 × 96 dynamic array chip and performed using BioMark HD system (Fluidigm, San, CA, USA). All primers for this array chip were obtained from QIAGEN (Venlo, The Netherlands) including nine control genes: RPL13A, BTF3, YWHAZ, UBE2D2, ATP6V1G1, IPO8, HBS1L, AHSP and TBP. Samples were measured in duplicates and analyzed using BioMark software, delivered with the HD system.

Whole transcriptome RNA sequencing

RNA sequencing was performed at BGI genomics (Hong Kong, People's Republic of China) following standard protocol established by BGI genomics. In short, total isolated RNA was enriched for mRNA using Oligo(dT) beads and generated fragments were size selected for amplification. Amplified fragments were quality controlled and sequenced using Illumina HiSeq 2000. Reads were aligned to a reference sequence using SOAPaligner/SOAP2. Gene expression was calculated using Reads Per Kilobase per Million mapped reads (RPKM) method [23].

Statistical analysis

Survival curves were calculated using the Kaplan–Meier method and P-values were calculated using the log-rank and Gehan Breslow Wilcoxon test using SPSS 20 (IBM Inc. Amsterdam, The Netherlands) and Prism Graphpad 6 (Graphpad Software Inc. La Jolla, CA, USA). Correlations were calculated with SPSS 20 using Spearman or Pearson correlation. High RNA expression was set as expression above the median. Student *t*-tests *P*-value was calculated using Prism Graphpad assuming non-parametric distribution due to limited numbers of samples and were corrected using Manley–Welch correction.

RESULTS

EWS expresses all *CXCR4–CXCR7* axis genes and tumor samples have an increased *CXCR4-1/CXCR4-2* ratio

RNA expression levels of chemokines and their receptors in cell lines were analyzed using both Fluidigm RT-Q-PCR and whole transcriptome analysis. Both methods showed comparable expression levels and that all genes involved in the *CXCR4–CXCR7* axis were expressed (**Figure 1**). We performed an expression analysis of a *CXCR4–CXCR7* axis chemokine and their receptor gene set, from which expression differences were observed for *CXCR7* and *CXCL12* between cell lines and tumor samples, using a panel of 18 therapy naïve tumor samples, 21 cell lines and 1 primary culture (**Tables 1A and 2**). The cell line RT-Q-PCR expression levels of the *CXCR4–CXCR7* axis genes were compared with expression levels in tumor samples and showed an increased expression of CXCL12 and CXCR7 in tumor samples. Furthermore, within the cell lines and among individual tumor samples a large variation was observed (**Figure 2A**).

Both splice variants of *CXCR4* were expressed in all tumor samples and cell lines except the A673 cell line and no significant difference was observed between the groups (**Figure 2B**). The ratio between splice variants has been shown to be functionally relevant, therefore we further analyzed the ratio between expression levels of *CXCR4-1* and *CXCR4-2* in our samples [24]. The *CXCR4-1/CXCR4-2* ratio was uniformly distributed in the cell line panel with two outliers; A673 cell line without *CXCR4-1* expression and COH cell line with a high *CXCR4-1/CXCR4-2* ratio (**Table S1**). Tumor samples of panel I demonstrated a wide distribution (range 0.06–0.003, SD = 0.015) and an overall significantly higher *CXCR4-1/CXCR4-2* ratio when it was compared to cell lines (median of 0.030 versus 0.012, $P < 0.001$) (**Figure 2C**).
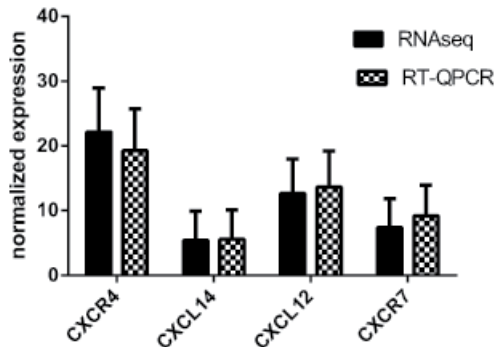
Figure 1: RT-Q-PCR and transcriptome analysis resulted in comparable expression levels of *CXCR4–CXCR7* genes using all studied samples. Housekeeping gene normalised RT-Q-PCR expression levels were measured in duplicates (mean ± SEM)

CXCR4-1 over *CXCR4-2* ratio, *CXCR7* and *CXCL14* expression associate with development of metastases and survival

The large observed variation in *CXCR4–CXCR7* axis genes and in the *CXCR4-1/CXCR4-2* between individual tumor samples prompted us to perform a comparison between patient samples. A survival analysis was performed using the *CXCR4–CXCR7* axis gene expressions

**Table 2. Ewing sarcoma cell lines and their origin**

Cell line	Sex	Age (years)	Tumor source	Translocation[#]	TP53 literature	TP53 status [#]	TP53 expression (RPKM)	CDKN2A expression (RPKM)
RM-82[a]	male	8	femur	EWS-ERG	p.Arg273His	rs28934576[*†]	79.78	54.99
CADO-ES-1[a]	female	19	malignant pleural effusion	EWS-ERG	wt	wt	26.79	-
TTC-466[a]	female	5	lung metastasis	EWS-ERG	NA	rs28934578[*]	63.06	81.28
IARC-EW-3[a]	male	14	malignant pleural effusion	EWS-ERG	c-852_858del	c-852_858del[†]	18.72	24.72
L-4027[c]	male	-	NA	EWS-ERG	NA	wt	65.4	-
STA-ET-10	NA	NA	NA	EWS-FEV	wt	wt	57.29	5.33
L-872[b]	male	20	Rib	EWS-FLI1 type I	c 641 A>G, p.H214R	chr17.7578.208 A > G [†]	47.37	19.35
L-1062[b]	male	17	femur	EWS-FLI1 type I	c 404 G > T, pC135F	chr17.7578526 G > T [†]	90.27	31.69
IARC-EW-7[a]	female	20	NA	EWS-FLI1 type I	NA	wt	48.35	1.04
TC-32[a]	female	17	pelvis bone marrow	EWS-FLI1 type I	NA	wt	99.81	-
TC-71[a]	male	23	humerus	EWS-FLI1 type I	p.Arg213X	missing exon 5,6,7	1.97	-
STA-ET-1[a]	female	13	humerus	EWS-FLI1 type I	wt	rs28934576[*] heterozygous	30.09	-
WE-68a	female	19	fibula	EWS-FLI1 type I	wt	wt	62.14	-
SK-NM-C[a]	female	14	supraorbital metastasis	EWS-FLI1 type I	c.17-_572del	c.17-_572del[†]	64.22	100.3
A-673[a]	male	15	NA	EWS-FLI1 type II	552insCA	NA	3.65	-
RD-ES[a]	male	19	humerus	EWS-FLI1 type II	p.Arg273Cys	rs121913343[*†]	62.06	24.29
SK-ES-1[a]	male	18	NA	EWS-FLI1 type II	p.Cys176Phe	chr17.7578403 G>T [†]	72.18	41.81
CHP-100[a]	female	12	mediastinum	EWS-FLI1 type II	wt	wt	3.25	45.13
6647[a]	NA	NA	NA	EWS-FLI1 type II	NA	rs28934573[*]	66.97	21.69
VH-64[a]	male	24	malignant pleural effusion	EWS-FLI1 type II	wt	wt	48.28	-
COH	NA	NA	femur	EWS-FLI1 type III	wt	wt	61.90	12.03

Translocation, TP53 status and CDKN2A expression were analysed using transcriptome profiling from this study. wt: wild type TP53; NA: Not available; RPKM: Reads Per Kilobase per Million mapped reads; -: lacking expression. [a]Described by van Valen [43]. [b] Characterized by K. Szuhai et al. [44]. [c]Primary culture. [†]Corresponding with literature described TP53 mutation. [*]Known pathogenic mutation in TP53. [#] Detected by whole transcriptome analysis
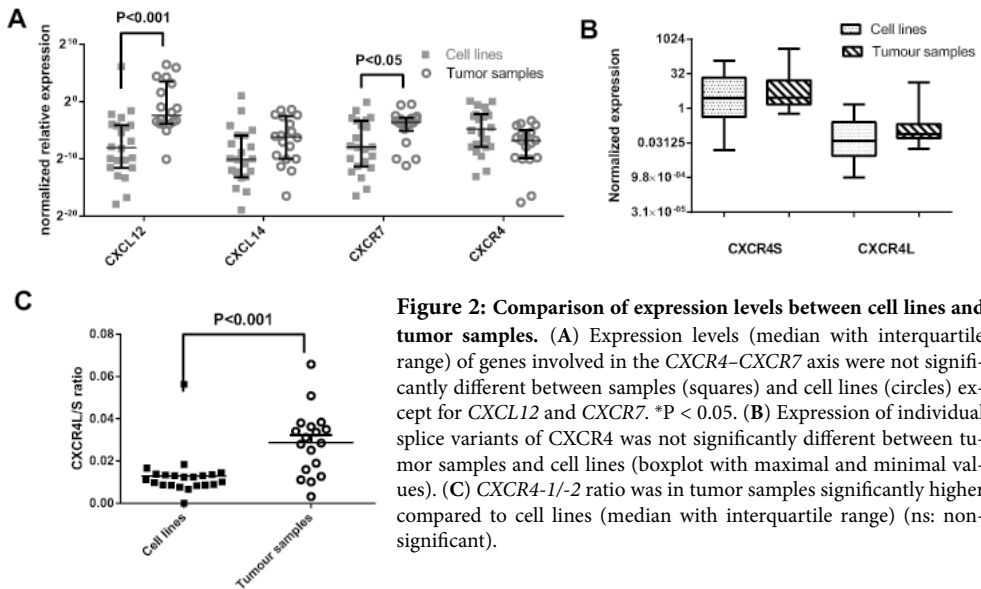
Figure 2: Comparison of expression levels between cell lines and tumor samples. (**A**) Expression levels (median with interquartile range) of genes involved in the *CXCR4–CXCR7* axis were not significantly different between samples (squares) and cell lines (circles) except for *CXCL12* and *CXCR7*. *P < 0.05. (**B**) Expression of individual splice variants of CXCR4 was not significantly different between tumor samples and cell lines (boxplot with maximal and minimal values). (**C**) *CXCR4-1/-2* ratio was in tumor samples significantly higher compared to cell lines (median with interquartile range) (ns: non-significant).

and the *CXCR4-1/CXCR4-2* ratio of the primary therapy-naïve tumor samples. We observed that a high *CXCR4-1/CXCR4-2* ratio and high expression of *CXCL14* and *CXCR7* correlated with an improved event free survival (EFS) ($P < 0.03$, $P < 0.01$, $P < 0.02$) and OS ($P < 0.03$, $P < 0.02$, $P < 0.01$), respectively (**Figure 3A-C, G-I**). Consistent with the correlations with improved survival were increased *CXCL14* ($P < 0.02$) and *CXCR7* ($P < 0.02$) expression negatively correlated with the development of metastasis. The results were validated with an independent second panel of 25 therapy-naïve tumor samples using the same methods (Table 1B; panel II). The same pattern of survival associations with improved EFS was observed for increased *CXCR4-1/CXCR4-2* ratio ($P < 0.05$) and expression of *CXCL14* ($P < 0.04$) (**Figure 3D,I**), while the expression of *CXCL14* ($P < 0.02$) and *CXCR7* ($P < 0.03$) showed a negative correlation with the development of metastasis. Expression of *CXCR7* was associated with improved EFS but did not reach a significant level (**Figure 3F**). No association to overall survival was observed in panel II (**Figure 3J–K**). Expression levels of *CXCR4* or *CXCL12* did not show significant correlation with survival in either panel. (**Figure S1A–H**). As control experiment a survival analysis was performed using the classical prognostic parameters tumor volume, metastasis at diagnosis, location and metastasis after diagnosis of both panels [25]. The development of metastasis after diagnosis was strongly associated with poor survival ($P < 0.01$) consistent with panel I. A pelvic located tumor correlated with a significant poor EFS and OS in panel I, while these were not significant in panel II. Intriguingly, metastasis at diagnosis did not correlate significantly with survival in both panels (**Figure S2**).
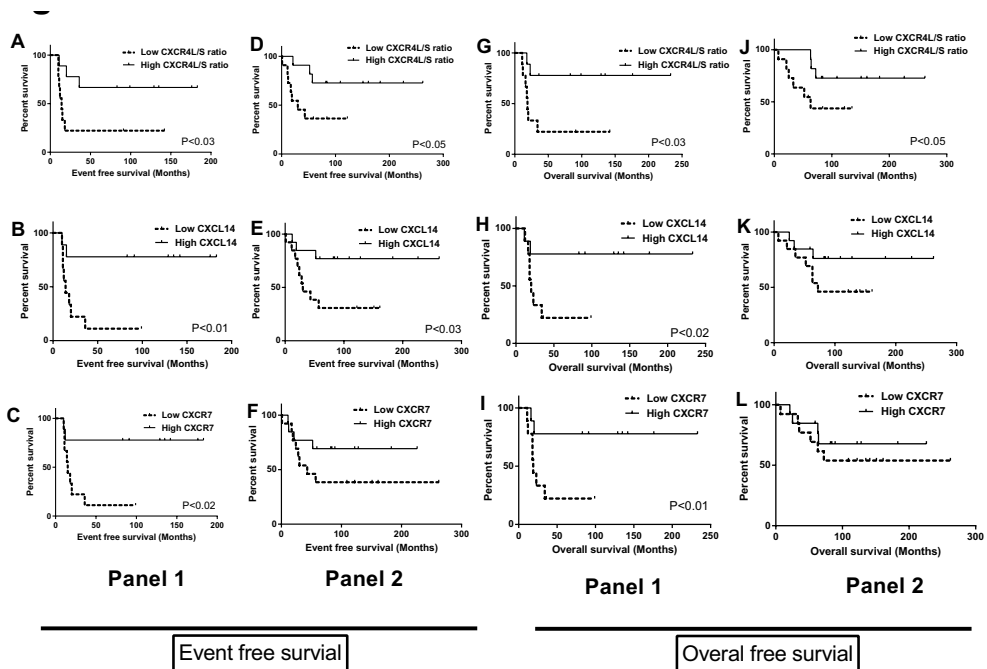
Figure 3: Overview of CXCR4–CXCR7 axis genes and event free survival (EFS), overall survival (OS) in panel 1 and panel 2. *CXCR4-1/-2* ratio and *CXCL14* expression were associated with a significant better EFS in both panels, *CXCR7* in panel I with OS in panel I. RNA expressions of the *CXCR4–CXCR7* axis genes of the therapy-naïve tumor samples of panel I (n = 18) (**A–C, G–I**) and panel II (n = 25) (**D–F, J–L**) were correlated using Kaplan–Meier survival analysis. Median was set as threshold between high (straight line, panel I n = 9, panel II n = 13) and low expression (dotted line, panel I n = 9, panel II n = 12). A significant association between high *CXCR4-1/CXCR4-2* ratio and improved EFS or OS was observed in both panels.

DISCUSSION

In earlier studies a crucial role of the CXCR4/CXCR7 axis in solid tumor development and prognosis has been reported [17, 19, 26]. Recent discoveries regarding the receptor–receptor and novel ligand–receptor interaction between CXCR4, CXCR7, CXCL12 and CXCL14 have been reported. Contradictory results in Ewing sarcoma prompted us to study the role of these chemokines in therapy-naïve patient material and cell lines [15, 16, 18]. In addition, we studied expression levels of the earlier reported CXCR4 isoforms in tumor samples as the expression of these isoforms in particular might partly be responsible for the contradictory results [15, 16, 20]. All chemokines and receptors of the *CXCR4–CXCR7* axis were expressed in EWS but a large variation was observed between individual samples, consistent with previous observations [16, 27]. The observed increased expression of *CXCR7* and *CXCL12* in tumor samples compared to cell lines could be stromal derived since both endothelial and perivascular cells express *CXCR7* and *CXCL12* and EWS is highly vascularized [28, 29]. In our results, increased expressions of *CXCL14*, *CXCR7* and *CXCR4-1/CXCR4-2* ratios were associated with better EFS and OS in panel I. In panel II increased *CXCL14* expression and *CXCR4-1/CXCR4-2* ratio were associated with better EFS. However, *CXCL12* and *CXCR4* mRNA expression levels did not correlate significantly with EFS or OS. In both panels there was an inverse correlation of increased expression of *CXCL14* and *CXCR7* and development of me-

tastases. This can be related to immune cell infiltration [30, 31]. Classical clinical parameters were included to compare with the newly identified parameters. In panel II none of the classical parameters were significant predictors of survival. This cohort has been extensively treated by different rescue protocols after failure of the initial treatment.

Contrary to our results, increased expression of CXCR4 or CXCR7 has been reported to be associated with poor survival in EWS and other tumors [16-17]. This might be attributed to different methodologies and patient groups used in different studies or might be related to biological effects between different tumor types. For example, the effect of CXCR4 and CXCR7 is dependent on their spatial–temporal distribution. When they are expressed in the same cell, heterodimers can be formed leading to an enhanced CXCR4 downstream signaling [26]. When CXCR7 is expressed alone it can act as scavenging receptor for CXCL12 and subsequently reduces CXCR4 activation by CXCL12 [32]. By flow cytometry and immunohistochemistry a heterogeneous CXCR4 expression has been shown in EWS and this may hold for CXCR7 as well [27]. The local tumor microenvironment can be an influencing factor here as well. CXCR7, CXCR4 and CXCL12 are expressed by tumor-associated vessels and immune cells, where CXCR7 is detected largely intracellular in immune cells [31]. Furthermore, infiltrating macrophages, for example, have been reported to predict a worse survival in classical Hodgkin's lymphoma and were associated with reduced metastasis and improved survival in high-grade osteosarcoma [33-34].

Based on our data the following model can be proposed (**Figure 4**): The paracrine and autocrine CXCR4 signaling present in EWS might be altered by CXCR4-1/-2 ratio, CXCL14 and CXCR7 expressions. High expression of CXCL14 antagonizes CXCL12 binding to CXCR4 and increased CXCR7 sequesters CXCL12 co-operatively leading to a reduced CXCR4 signaling [18, 32]. The investigated CXCR4 isoforms might be present in dimers or oligomers. The presence of CXCR4-1 in these complexes could lead to down regulation of CXCR4 signaling as it has been shown in rat basal leukemia 2H3 cells [20]. Moreover, the CXCR4-1 isoform may have a higher affinity for CXCL14 than CXCR4-2, consequently further increasing the antagonizing effect of CXCL14 [18].

Hence, CXCR4 signaling is a potential targetable pathway and inhibition of CXCR4 signaling in EWS *in vitro* and in xenografts has already been shown to reduce tumor migration growth and angiogenesis [15, 27, 35]. Potential drugs to treat EWS are; CXCL12 neutralizing ligands, like chalcone 4, CXCR4 antagonists, like AMD3100 and CXCL14 analogues (**Figure 4**) [19, 36-37].

Here we document that the increased expression of genes involved in the down regulation of CXCR4 signaling and the CXCR4 splice variant balance predict the prognosis of therapy-naïve Ewing sarcoma patients. In addition the *CXCR4-1/-2 ratio*, the level of *CXCL14* and level of *CXCR7* may be used as markers for therapeutic inhibition of the CXCR4 pathway. Based on our results, additional studies to further characterize the role of altered CXCL14, CXCR7 and CXCR4-1/-2 ratio in CXCR4 signaling, could be performed in model systems, such as well-established zebrafish models [38].

ACKNOWLEDGEMENTS
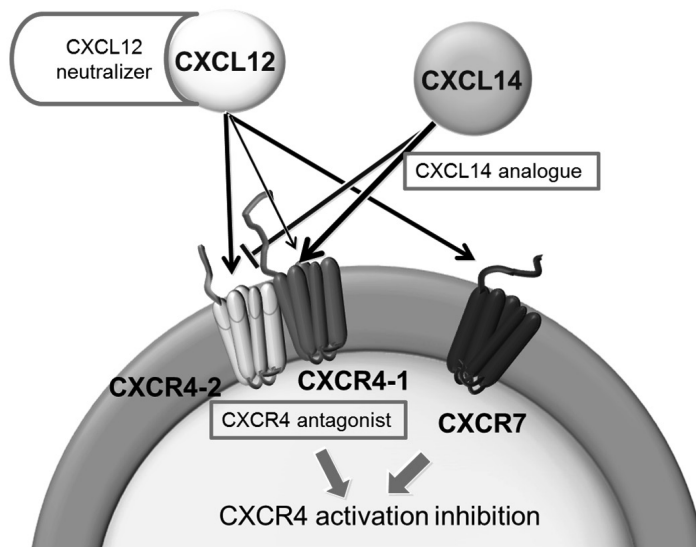
Figure 4: Model for CXCR4 signaling in Ewing sarcoma: CXCL12 binds and activates CXCR4-2, which is inhibited by CXCL14 and CXCR7 by inhibiting receptor binding and scavenging of CXCL12. Dimerization of CXCR4-1 and CXCR4-2 results in CXCR4 activation inhibition due to either change in CXCR4-2 signalling or by higher CXCR4-1 affinity for CXCL14. As available therapeutic options (boxed) are CXCL14 analogues, CXCL12 neutralizers and CXCR4 inhibitors (see [19, 36-37]).

REFERENCES

1   De Alava, E., Lessnick, S. L. & Sorensen, P. H. in *WHO Classification of Tumors of Soft Tissue and Bone* (eds C.D.M. Fletcher, J.A. Bridge, P. C. W. Hogendoorn, & F. Mertens) 306-9 (IARC, 2013).

2   Sand, L. G. L., Szuhai, K. & Hogendoorn, P. C. W. Sequencing overview of Ewing sarcoma: a journey across genomic, epigenomic and transcriptomic landscapes. *Int J Mol Sci* **16**, 16176-215, (2015).

3   Pierron, G. *et al.* A new subtype of bone sarcoma defined by BCOR-CCNB3 gene fusion. *Nat Genet* **44**, 461-6, (2012).

4   Szuhai, K. *et al.* The NFATc2 Gene Is Involved in a Novel Cloned Translocation in a Ewing sarcoma Variant That Couples Its Function in Immunology to Oncology. *Clin Cancer Res* **15**, 2259-68, (2009).

5   Graham, C., Chilton-MacNeill, S., Zielenska, M. & Somers, G. R. The CIC-DUX4 fusion transcript is present in a subgroup of pediatric primitive round cell sarcomas. *Hum Pathol* **43**, 180-9, (2012).

6   Balamuth, N. J. & Womer, R. B. Ewing's sarcoma. *Lancet Oncol* **11**, 184-92, (2010).

7   Le Deley, M.-C. *et al.* Impact of EWS-ETS Fusion Type on Disease Progression in Ewing's sarcoma/peripheral primitive neuroectodermal tumor: Prospective Results From the Cooperative Euro-EWING 99 Trial. *J Clin Oncol* **28**, 1982-8, (2010).

8   Bacci, G. *et al.* Therapy and survival after recurrence of Ewing's tumors: the Rizzoli experience in 195 patients treated with adjuvant and neoadjuvant chemotherapy from 1979 to 1997. *Ann Oncol* **14**, 1654-9, (2003).

9   Ladenstein, R. *et al.* Primary disseminated multifocal Ewing sarcoma: results of the Euro-EWING 99 trial. *J Clin Oncol* **28**, 3284-91, (2010).

10   van Maldegem, A., Hogendoorn, P. & Hassan, A. The clinical use of biomarkers as prognostic factors in Ewing sarcoma. *Clin Sarc Res* **2**, 7, (2012).

11   Ewing, J. Diffuse endothelioma of bone *Proc New York Path Soc* **21**, 17-24, (1921).

12   DuBois, S. G., Marina, N. & Glade-Bender, J. Angiogenesis and vascular targeting in Ewing sarcoma. *Cancer* **116**, 749-57, (2010).

13   Pardali, E. *et al.* Critical role of endoglin in tumor cell plasticity of Ewing sarcoma and melanoma. *Oncogene* **30**, 334-45, (2011).

14   Bühnemann, C. *et al.* Quantification of the Heterogeneity of Prognostic Cellular Biomarkers in Ewing sarcoma Using Automated Image and Random Survival Forest Analysis. *PLoS One* **9**, e107105, (2014).

15   Berghuis, D. *et al.* The CXCR4-CXCL12 axis in Ewing sarcoma: promotion of tumor growth rather than metastatic disease. *Clin Sarc Res* **2**, 24, (2012).

16   Bennani-Baiti, I. M. *et al.* Intercohort Gene Expression Co-Analysis Reveals Chemokine Receptors as Prognostic Indicators in Ewing's sarcoma. *Clin Cancer Res* **16**, 3769-78, (2010).

17   Lippitz, B. E. Cytokine patterns in patients with cancer: a systematic review. *Lancet Oncol* **14**, e218-e28, (2013).

18   Tanegashima, K. *et al.* CXCL14 is a natural inhibitor of the CXCL12–CXCR4 signaling axis. *FEBS Lett* **587**, 1731-5, (2013).

19   Domanska, U. M. *et al.* A review on CXCR4/CXCL12 axis in oncology: No place to hide. *Eur J Cancer* **49**, 219-30, (2013).

20   Gupta, S. K. & Pillarisetti, K. Cutting Edge: CXCR4-Lo: Molecular Cloning and Functional Expression of a Novel Human CXCR4 Splice Variant. *J Immunol* **163**, 2368-72, (1999).

21   Tamamis, P. & Floudas, C. A. Elucidating a Key Component of Cancer Metastasis: CXCL12 (SDF-1α) Binding to CXCR4. *J Chem Inf Model* **54**, 1174-88, (2014).

22   van Kuppeveld, F. J. *et al.* Genus- and species-specific identification of mycoplasmas by 16S rRNA amplification. *Appl Environ Microbiol* **58**, 2606-15, (1992).

23   Mortazavi, A., Williams, B. A., McCue, K., Schaeffer, L. & Wold, B. Mapping and quantifying mammalian transcriptomes by RNA-Seq. *Nat Meth* **5**, 621-8, (2008).

24   Bates, D. O. *et al.* Association between VEGF Splice Isoforms and Progression-Free Survival in Metastatic Colorectal Cancer Patients Treated with Bevacizumab. *Clin Cancer Res* **18**, 6384-91, (2012).

25   Hogendoorn, P. C. W. *et al.* Bone sarcomas: ESMO Clinical Practice Guidelines for diagnosis, treatment and follow-up. *Ann Oncol* **21**, v204-v13, (2010).

26   Décaillot, F. M. *et al.* CXCR7/CXCR4 Heterodimer Constitutively Recruits β-Arrestin to Enhance Cell Migration. *J Biol Chem* **286**, 32188-97, (2011).

27   Krook, M. A. *et al.* Stress-induced CXCR4 Promotes Migration and Invasion of Ewing Sarcoma. *Molecular Cancer Research*, (2014).

28   Ding, L. & Morrison, S. J. Haematopoietic stem cells and early lymphoid progenitors occupy distinct bone marrow niches. *Nature* **495**, 231-5, (2013).

29   Berahovich, R. D. *et al.* Endothelial expression of CXCR7 and the regulation of systemic CXCL12 levels. *Immunology* **141**, 111-22, (2014).

30   Rivera, Lee B. *et al.* Intratumoral Myeloid Cells Regulate Responsiveness and Resistance to Antiangiogenic Therapy. *Cell Rep* **11**, 577-91, (2015).

31   Sánchez-Martín, L., Sánchez-Mateos, P. & Cabañas, C. CXCR7 impact on CXCL12 biology and disease. *Trends Mol Med* **19**, 12-22, (2013).

32   Hoffmann, F. *et al.* Rapid Uptake and Degradation of CXCL12 Depend on CXCR7 Carboxyl-terminal Serine/Threonine Residues. *J Biol Chem* **287**, 28362-77, (2012).

33   Steidl, C. *et al.* Tumor-Associated Macrophages and Survival in Classic Hodgkin's Lymphoma. *N Engl J Med* **362**, 875-85, (2010).

34   Buddingh, E. P. *et al.* Tumor-Infiltrating Macrophages Are Associated with Metastasis Suppression in High-Grade Osteosarcoma: A Rationale for Treatment with Macrophage Activating Agents. *Clin Cancer Res* **17**, 2110-9, (2011).

35   Hamdan, R., Zhou, Z. & Kleinerman, E. S. Blocking SDF-1α/CXCR4 Downregulates PDGF-B and Inhibits Bone Marrow–Derived Pericyte Differentiation and Tumor Vascular Expansion in Ewing Tumors. *Molecular Cancer Therapeutics*, (2013).

36   Daubeuf, F. *et al.* An Antedrug of the CXCL12 Neutraligand Blocks Experimental Allergic Asthma without Systemic Effect in Mice. *J Biol Chem* **288**, 11865-76, (2013).

37   Tanegashima, K. *et al.* Dimeric peptides of the C-terminal region of CXCL14 function as CXCL12 inhibitors. *FEBS Lett* **587**, 3770-5, (2013).

38   van der Ent, W. *et al.* Ewing sarcoma inhibition by disruption of EWSR1–FLI1 transcriptional activity and reactivation of p53. *J Pathol* **233**, 415-24, (2014).

4

SUPPLEMENTARY DATA
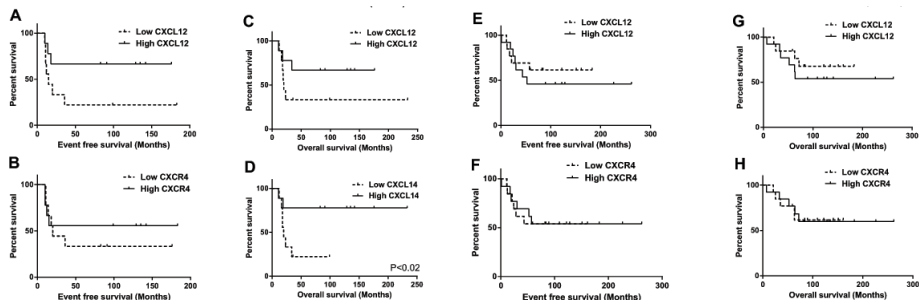
Figure S1: EFS and OS analysis of *CXCR4* and *CXCL12* of panel I and panel II. Kaplan-Meijer survival analysis of panel I (**A-D**) and panel II (**E-H**) for OS and EFS association with *CXCL12* and *CXCR4* expression levels. None of them were significantly associated with OS or EFS. A straight line corresponds to a high ratio or expression and a dotted line is low ratio or expression.
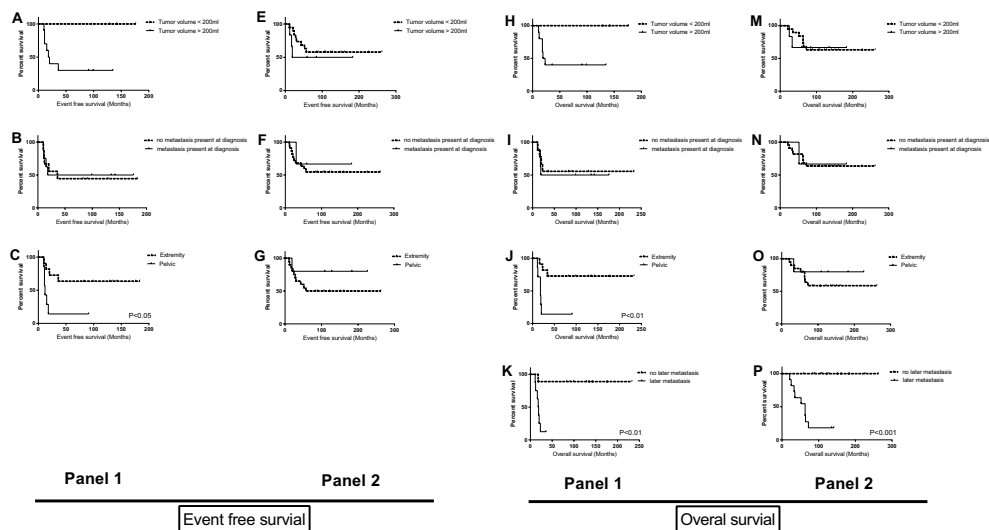
Figure S2: EFS and OS analysis of classical parameters of panel I and panel II. Kaplan-Meijer survival analysis of panel I (**A-C,H-K**) and panel II (**D-F,L-P**) for OS and EFS association with classical parameters; tumor volume, metastasis at diagnosis, tumor location at diagnosis and only OS association with development of later metastasis. Pelvic location of primary tumor at diagnosis was only in panel I significant. Development of later metastasis was highly significant in both panel I and panel II.

Table S1: Normalized expression of *CXCR4-2* and *CXCR4-1* and ratio between *CXCR4-1* and *CXCR4-2*

Cell lines	Expression		
	CXCR4-2	*CXCR4-1*	*CXCR4-1/-2*
L-1062	3.877	0.052	0.013
6647	33.314	0.284	0.009
CHP-100	48.492	0.406	0.008
RM-82	0.426	0.004	0.008
A-673	0.015	0.000	0.000
IARC-EW-7	1.074	0.007	0.007
SK-ES-1	0.180	0.002	0.011
L-4027	3.009	0.039	0.013
WE-68	17.255	0.213	0.012
L-872	1.057	0.010	0.010
IARC-EW-3	120.196	1.493	0.012
STA-ET-2.1	0.421	0.006	0.014
TTC-466	1.858	0.024	0.013
TC-32	56.346	0.937	0.017
STA-ET-10	6.658	0.059	0.009
SK-NM-C	1.077	0.015	0.014
CADO-ES1	52.325	0.962	0.018
STA-ET-1	10.085	0.101	0.010
TC-71	0.130	0.001	0.008
RD-ES	5.449	0.079	0.014
COH	0.219	0.012	0.056
VH-64	2.536	0.022	0.009

4